

## Morphology of the two unnamed seamounts in the Arabian Basin and their probable tectonic implications

C. M. Bijesh<sup>1,2</sup> and P. John Kurian<sup>1,\*</sup>

<sup>1</sup>National Centre for Polar and Ocean Research, Vasco da Gama, Goa 403 804, India

<sup>2</sup>School of Earth, Ocean and Atmospheric Sciences, Goa University, Taleigao Plateau, Goa 403 206, India

Newly acquired high resolution multibeam bathymetry data collected from Eastern Arabian Sea show the presence of two distinct, isolated seamounts (~27 km apart) in the flat Arabian Basin, west of Laccadive–Chagos Ridge. The seamount S1 with a relief of 1980 m from the adjacent seafloor has a linear ridge-like shape with NNE–SSW trend and is associated with craters and knolls near its base. Seamount S2 with a relief of 1830 m is conical in shape with steep slopes. Seismic characteristics imply that these two seamounts are extrusive volcanic features covered by thick pile of sediments along the flanks. The evolutionary history of the Arabian Basin and the tectonic fabric of the study area suggest that emplacement of the identified seamounts might be due to the Réunion hotspot volcanism.

**Keywords:** Morphology, multibeam bathymetry, Réunion hotspot volcanism, seamounts.

SEAMOUNTS are defined as the distinct, generally equidimensional elevations reaching or having heights greater than 1000 m above the surrounding seafloor relief as measured from the deepest isobaths that surrounds most of the feature<sup>1</sup>. Detailed mapping and systematic study of seamounts and other seabed features gain substantial momentum with the advancement of sonar technologies during the last couple of decades. Apart from this, satellite altimetry and global bathymetry data have been extensively used for the identification of seamounts in the world ocean and it is estimated that over 100,000 seamounts of height >1 km remain uncharted in the global oceans<sup>2</sup>. Study of seamounts assumes significance as they play an important role in fluid dynamics and mixing processes in ocean and also in sediment transportation and distribution<sup>3,4</sup>. These features can act as platform for biological productivity resulting in the formation of marine habitats, hence highly significant in marine ecosystem studies. It was also observed that topographical highs facilitate accumulation of mineral deposits having economic significance<sup>5,6</sup>. Seamounts also provide good record of crustal plate movement over hotspot and document the evolutionary history of ocean basins.

Sparse coverage of the seafloor using modern mapping tools resulted in identification of very few seamounts in the Arabian Sea<sup>7–9</sup>. Recently three seamounts were identified from the analysis of satellite-derived gravity data in the Arabian Basin<sup>10</sup>. As a part of the seabed mapping programme by the National Centre for Polar and Ocean Research (NCPOR), multibeam bathymetric mapping of the Western offshore region of India was carried out and these studies brought out several new seabed features, few of which were already reported<sup>11</sup>. In this communication, we present two isolated unnamed seamounts located in the Arabian Basin, west of Laccadive–Chagos Ridge (LCR, Figure 1) using high-resolution multibeam bathymetry data. The multibeam bathymetry data were

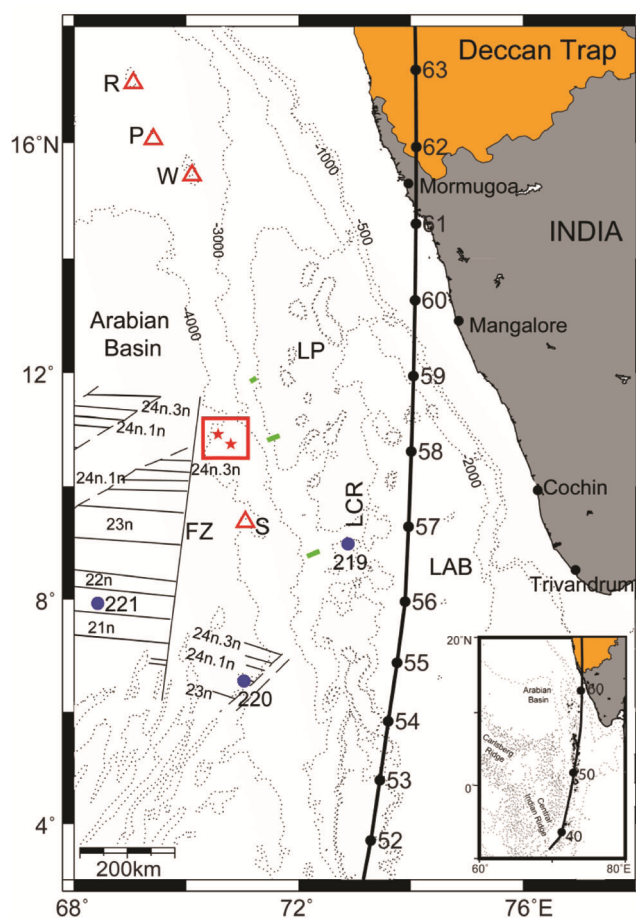


**Figure 1.** Generalized map of the southwestern continental margin of India and the adjoining deep offshore regions showing the major tectonic features and the location of the study area (red box, inset shows the regional tectonic settings with Réunion hotspot track in black thick line). Red solid asterisk symbols are the location of the seamounts described in the present study. Black dotted lines are selected (500 m, 1000 m, 2000 m, 3000 m and 4000 m) isobaths from GEBCO digital data set. The thick black line connecting the black solid circles represents the Réunion hotspot track<sup>24</sup>. The numbers given to the solid black circles represent the ages in million years (Ma). Blue solid circles are locations of DSDP sites. Green marks indicate the locations of SDRs<sup>20</sup>. LCR, Laccadive–Chagos Ridge; LP, Laccadive Plateau; FZ, Fracture zones; R, Raman Seamount; P, Panikkar Seamount; W, Wadia Guyot; S, Sagar Kanya Seamount.

\*For correspondence. (e-mail: john@ncpor.res.in)

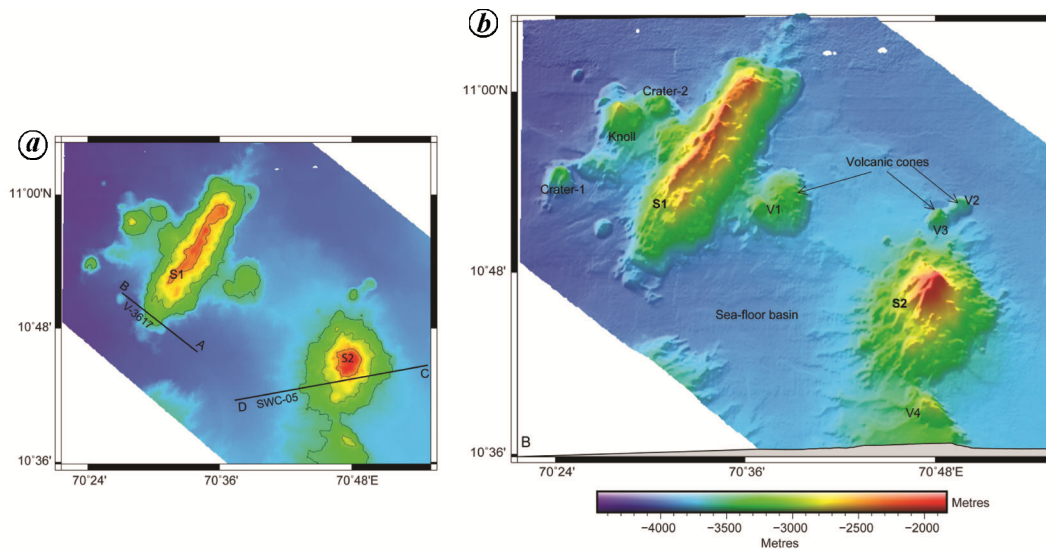


**Figure 2.** Filled contour map (a) and 3D perspective image (b) of the study area representing newly identified seamounts. S1, Seamount 1; S2, Seamount 2. Black thick lines in Figure 2a represent the locations of seismic section presented in Figure 5.

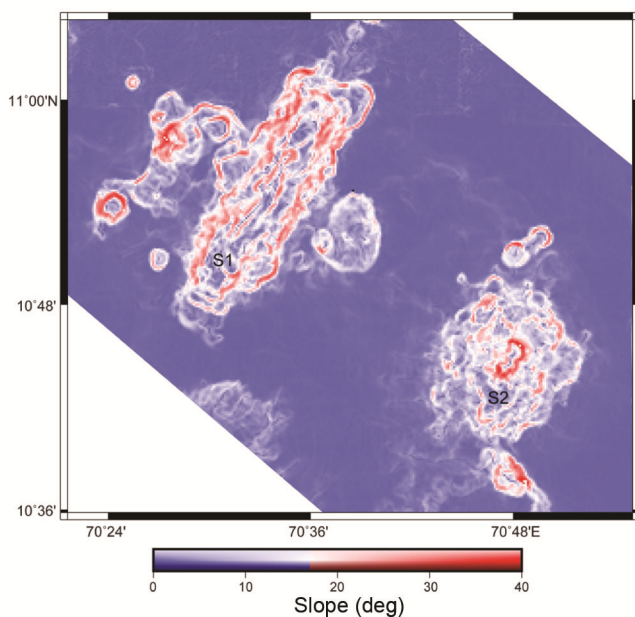


**Figure 3.** Slope map of the study area (in degrees) derived from the bathymetry data.

acquired onboard *RV MGS Sagar* during 2015 with Reson SeaBat 7150 multibeam echosounder operated at a frequency of 12 kHz. The navigation was guided using differential global positioning system (DGPS) and survey tracks were planned in such a way that adjacent swaths of multibeam swaths overlap at least 50%, thereby providing 100% insonification of the seafloor. Sound velocity profiles were collected at regular intervals and were applied to the multibeam data in real time for compensating variation in sound velocity in the water column. Manual

de-spiking (removal of erroneous depth measurement) in the bathymetry data was undertaken using Caris 'Hips and Sips' software during post processing. Finally, the processed data were used to create a digital terrain model with a grid spacing of 100 m. Apart from the multibeam bathymetry data, available single channel seismic section and multichannel seismic (MCS) section were also used during the present study for characterizing the seamounts.

Bathymetric contour maps, 3D bathymetry images and slope angle maps (Figures 2a, b and 3 respectively) were prepared to infer and exemplify morphological characteristics of the area. Analyses of the data reveal the presence of two isolated unnamed seamounts, S1 and S2, in the region. S1 is located at 70.567°E, 10.921°N situated in a water depth of 4080 m with a NNE–SSW trend. The summit part of S1 lies at a depth of 2100 m resulting in a height of 1980 m from the seafloor. The summit area of S1 has rough topography with linear ridge-like shape (Figures 2 and 3). S1 has a basal extent of ~33.3 km and width of ~13.2 km which occupies an area ~438 sq. km on the seafloor. Slope of the flanks is moderate to high in both the directions of S1 (~20° to 35° in Figure 4). Near the western flank of S1, a significant morphological feature is observed with a relief of 740 m, rounded profile, spatial extent much less than S1 and is referred to as 'knoll'<sup>1</sup> (Figure 2). Adjacent to this, two annular and partially collapsed volcanic features are identified, which are referred to as 'crater' (Figures 2 and 3). Both craters are almost similar in physical dimension with a diameter of ~1.5 km. These exhibit a prominent depression in the centre and its rim is demarcated in the slope map with a high value followed by low values in the central part (Figure 3). A prominent elevation with a conical shape

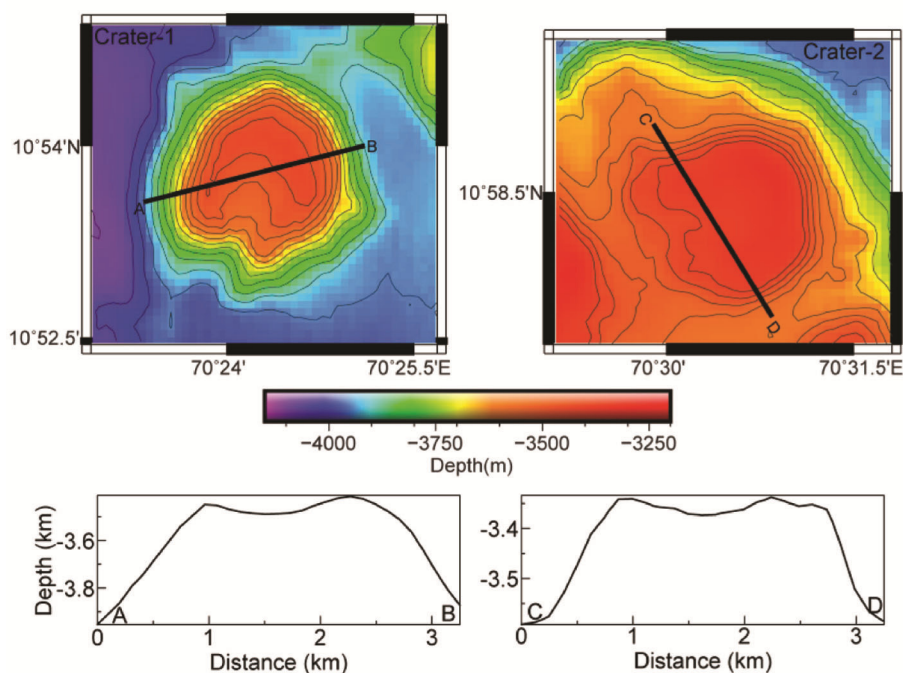


**Figure 4.** Bathymetric images of the craters (crater-1 and 2 in Figure 2) and respective bathymetric profiles (AB and CD) over the feature.

(marked as volcanic cone V1 in Figure 2) is observed on the eastern side of S1. Approximately 27 km away in southeast direction from S1 another seamount S2 has been identified from the bathymetry data (Figure 2). Summit of the seamount S2 is with a limited areal extent and exhibits a conical shape. The centre location of seamount S2 is identified at 70.794°E, 10.747°N. S2 is situated over a flat seafloor of about 3660 m water depth and seamount summit is at 1830 m thus giving a relief of 1830 m. The basal length and width are 18.8 km, 14.8 km respectively, and thus occupies an area of ~278 sq. km on the seafloor. S2 exhibits steep slopes (25°–30°) along the flanks up to 2300 m water depth and moderate to high slope afterwards (Figures 2 and 3). Volcanic cones are identified adjacent to the seamount S2 (V2, V3 and V4 in Figure 2) altogether resembling a chain-like appearance. There are similarities in a few of the morphological characteristics of these seamounts, such as, terrace-like feature is observed around 2600 m to 2800 m water depth on S1 and 2600 m to 2900 m water depth in case of S2. Also, gully-like patterns are observed over the flanks of both the seamounts. The terrace-like features and gully patterns might have been formed due to the erosional processes.

Publicly available single channel seismic section (V-3617 from GeoMapApp) which cut across the seamount S1 at the southern edge (Figure 5a) and multichannel seismic (MCS) section (SWC-05) collected by Directorate General of Hydrocarbon (DGH), which cut across seamount S2 (Figure 5b) are utilized during the present

study (Figure 2a for the location of seismic sections). As inferred from V-3617, the flanks of S1 are covered with thick sediments of ~0.5–0.6 s (TWT) (Figure 5a). MCS data reveal that seamount S2 possesses steep flanks and sedimentary layer is negligible or absent on the top (Figure 5b). The flanks are covered with a 0.4–0.5 s (TWT) thick sedimentation and exhibit high amplitude discontinuous reflection characteristics. Reflections are broken and chaotic beneath the seamount. The basement of seamounts S1 and S2 has similar seismic signatures and appear as volcanic extrusive.

Qualitative analysis of the MB data was carried out with global bathymetry grids from GEBCO<sup>12</sup> and SRTM30\_PLUS<sup>13</sup> to assess the quality of global grids vis-à-vis shipboard swath bathymetry data. Morphology of seamounts S1 and S2 deduced from MB data exhibits a significant change from the global bathymetry grids in terms of the trend of S1, distinctly identifiable features (e.g. craters, knoll, volcanic cone) associated with seamounts, shape of the seamounts, its areal extension and total height of the seamounts (Figure 6).

Generally, process of formation of seamounts is debatable and several hypotheses were put forward on the seamount genesis, such as hotspot–ridge interaction, ridge parallel faulting, off-axis volcanism, propagating fracture and hotspot activity, depending on the geological settings. With the aid of the newly acquired MBES data, seismic data and presently available geophysical and geological constraints, we attempt to give a reasonable hypothesis on the genesis of the identified seamounts.



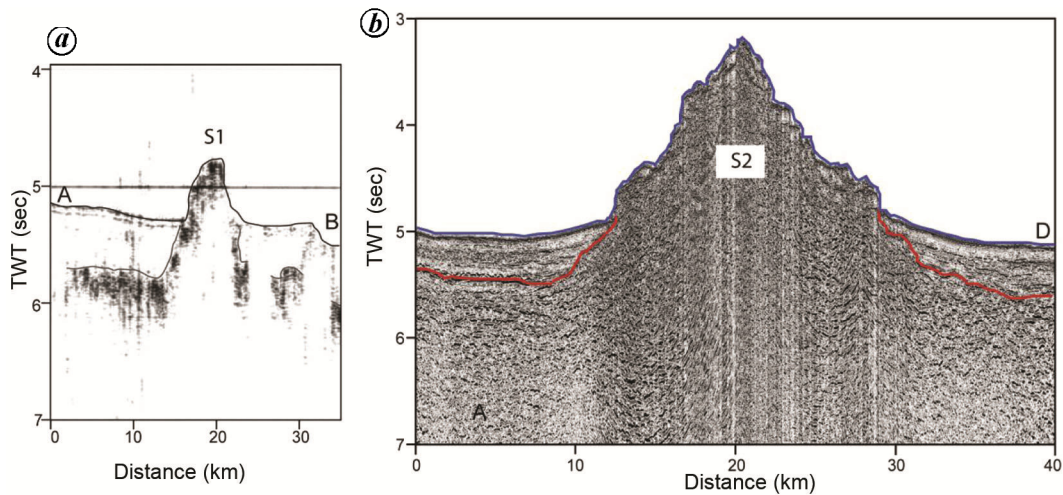


**Figure 5.** Images of seismic section along the (a) seamount S1, (b) seamount S2. Location of the sections is given in Figure 2a.

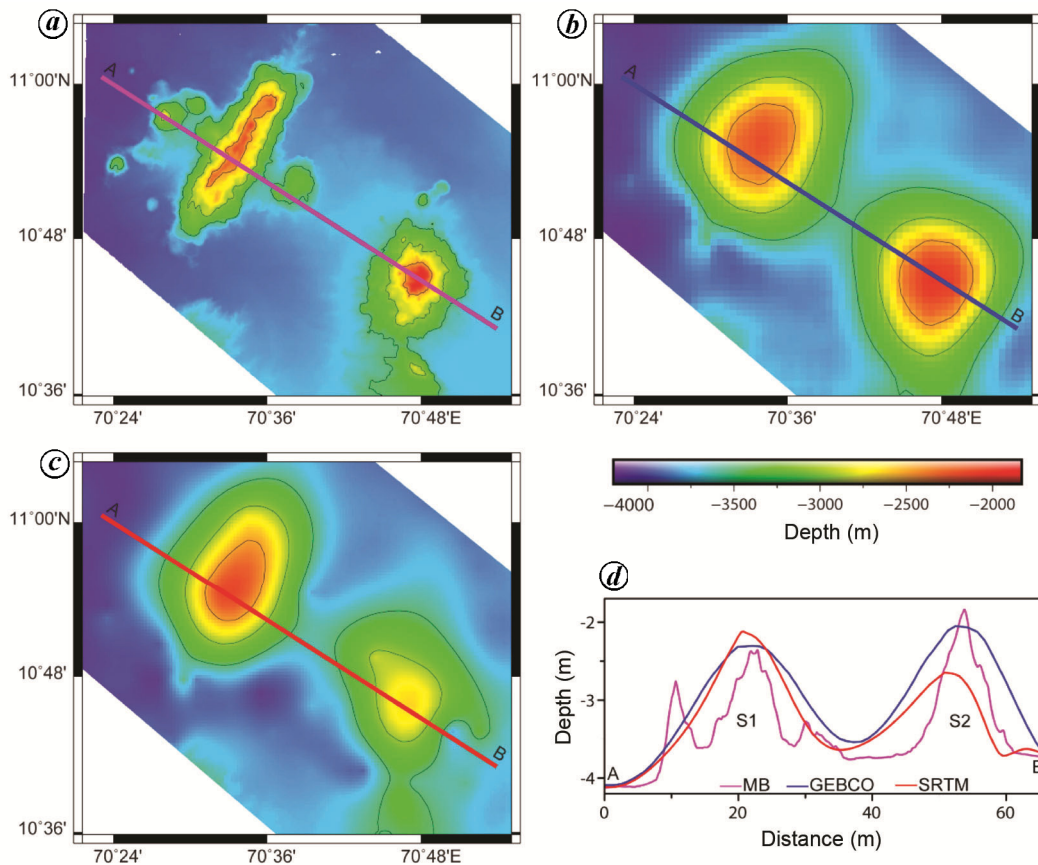


**Figure 6.** Filled contour maps of (a) MB data, (b) GEBCO, (c) SRTM for the same geographical extent. d. Bathymetric profiles taken for MB, GEBCO and SRTM and the location of profiles is given in the respective contour maps.

Previous studies suggest that a major portion of the Arabian Sea, westward of the Laccadive and Laxmi ridges, was formed by seafloor spreading along the Carlsberg Ridge in two discrete episodes<sup>14-16</sup>. The initial spreading of these two phases started during Early

Tertiary when the spreading centre jumped between India and Seychelles blocks. Réunion hotspot volcanism which was active in the Indian subcontinent province between 68 and 62 Ma is considered as the triggering mechanism for the separation of India and Laxmi-Seychelles block<sup>17</sup>,

which caused formation of massive Deccan flood basalt. The Réunion hotspot volcanism also had an intense influence on the oceanic crust, as Indian plate moved towards north over the hotspot. The formation of Laxmi Basin seamount chain identified in the axial part of Laxmi Basin is considered to be the consequence of an anomalous volcanic activity due to the interaction of Réunion hotspot with extinct Laxmi Basin spreading centre<sup>8</sup>. Recently identified seamounts, hills and knolls in the eastern part of LCR and Laccadive Plateau (LP) are also well correlated with the Réunion hotspot volcanism experienced in this region<sup>11</sup>. The origin of the seamounts identified in the Arabian Basin, west of the present study area, in the proximity of pseudofaults and fracture zones is correlated with the magma upwelling during the rift propagation<sup>10</sup>. Another important observation is regarding the nature of the crust in the study region. The identified spreading anomalies close to the newly mapped seamounts restricted by the fracture zone<sup>18</sup> indicate the oceanic nature for the crust. The DSDP sites in the proximity of the study area revealed the basaltic nature for the basement (DSDP sites 220, 221) and maximum age of Late Palaeocene for the sediments encountered (DSDP site 219)<sup>19</sup>. Also, seaward dipping reflectors (SDRs) identified in the western flank of the LCR imply occurrence of extrusive volcanism and continent–ocean boundary in the western limit of the LCR<sup>20</sup>.

Considering all these previous findings and the tectonic fabrics of the study region, two possibilities exist for the emplacement of the seamounts: hotspot volcanism and ridge–hotspot interaction. The seamounts are located in the eastern side of the fracture zone where no magnetic anomaly has been identified. Also, the formation of the Sagar Kanya Seamount, south of the study area (Figure 1), is attributed to the Réunion hotspot volcanism (~58 Ma)<sup>7</sup>. In addition, the effect of the hotspot can influence more than 750 km distance<sup>21,22</sup> from the source. Hence, it is reasonable to correlate the emplacement of the seamounts to the Réunion hotspot volcanism. However, precise geological sampling and analysis from the seamounts are required for the proper understanding on the age constraints. Here we have qualitatively assessed the possible timing of the emplacement for the seamounts by considering the above mentioned geophysical constraints. The age of 24n.3n anomaly close to the seamounts is ~53–56 Ma (ref. 23) and hence the oceanic crust in the north of 24n.3n anomaly will be older than ~53 Ma. The computer modelled Réunion hotspot track<sup>24</sup> in Figure 1, which is running parallel to the seamounts, shows that the possibility of emplacement of the seamounts might be due to the hotspot volcanism. The emplacement of seamount might have taken place during the hotspot activity at ~53 Ma.

1. IOC-IHO, Standardization of undersea feature names, Publication B-6, 2013, 4.1 edn, p. 18.

2. Wessel, P., Sandwell, D. T. and S.-S. K., The global seamount census. *Oceanography*, 2010, **23**, 24–33.
3. Turnewitsch, R., Falahat, S., Nycander, J., Dale, A., Scott, R. B. and Furnival, D., Deep-sea fluid and sediment dynamics – influence of hill to seamount-scale sea floor topography. *Earth-Sci. Rev.*, 2013, **127**, 203–241.
4. Rivera, J. *et al.*, Morphometry of conception bank: evidence of geological and biological processes on a large volcanic seamount of the Canary Islands Seamount Province. *PLoS ONE*, 2016, **11**, 1–33.
5. Kodagali, V. N. and Sudhakar, M., Manganese nodule distribution in different topographic domains of the Central Indian Basin. *Mar. Georesour. Geotechnol.*, 1993, **11**, 293–309.
6. Sarma, K. V. L. N. S., Ramana, M. V., Subrahmanyam, V., Krishna, K. S., Ramprasad, T. and Desa, M., Seamounts an additional tool to confirm the nature of the crust and to locate possible mineral resources for dredging. *Mar. Georesour. Geotechnol.*, 1998, **16**, 41–51.
7. Bhattacharya, G. C. and Subrahmanyam, V., Geophysical study of a seamount located on the continental margin of India. *Geo-Marine Lett.*, 1991, **11**, 71–78.
8. Bhattacharya, G. C., Murty, G. P. S., Srinivas, K., Chaubey, A. K., Sudhakar, T. and Nair, R. R., Swath bathymetric investigation of the seamounts located in the laxmi basin, eastern arabian sea. *Mar. Geod.*, 1994, **17**, 169–182.
9. Mukhopadhyay, R., Rajesh, M., De, S., Chakraborty, B. and Jauhari, P., Structural highs on the western continental slope of India: Implications for regional tectonics. *Geomorphology*, 2008, **96**, 48–61.
10. Sreejith, K. M., Chaubey, A. K., Mishra, A., Kumar, S. and Rajawat, A. S., Pseudofaults and associated seamounts in the conjugate Arabian and Eastern Somali basins, NW Indian Ocean – New constraints from high-resolution satellite-derived gravity data. *J. Asian Earth Sci.*, 2016, **131**, 1–11.
11. Bijesh, C. M., John Kurian, P., Yatheesh, V., Tyagi, A. and Twinkle, D., Morphotectonic characteristics, distribution and probable genesis of bathymetric highs off southwest coast of India. *Geomorphology*, 2018, **315**, 33–44.
12. Weatherall, P. *et al.*, A new digital bathymetric model of the world's oceans. *Earth Sp. Sci.*, 2015, **2**, 331–345.
13. Becker, J. J. *et al.*, Global bathymetry and elevation data at 30 arc seconds resolution: SRTM30\_PLUS. *Mar. Geod.*, 2009, **32**, 355–371.
14. McKenzie, D. and Sclater, J. G., The evolution of the Indian Ocean since the Late Cretaceous. *Geophys. J. Int.*, 1971, **24**, 437–528.
15. Norton, I. O. and Sclater, J. G., A model for the evolution of the Indian Ocean and the breakup of Gondwanaland. *J. Geophys. Res. Solid Earth*, 1979, **84**, 6803–6830.
16. Miles, P. R. and Roest, W. R., Earliest sea-floor spreading magnetic anomalies in the north Arabian Sea and the ocean-continent transition. *Geophys. J. Int.*, 1993, **115**, 1025–1031.
17. Chaubey, A. K., Bhattacharya, G. C., Murty, G. P. S. and Desa, M., Spreading history of the Arabian Sea: some new constraints. *Mar. Geol.*, 1993, **112**, 343–352.
18. Chaubey, A. K., Dymant, J., Bhattacharya, G. C., Royer, J.-Y., Srinivas, K. and Yatheesh, V., Paleogene magnetic isochrons and palaeo-propagators in the Arabian and Eastern Somali basins, NW Indian Ocean. *Geol. Soc. London, Spec. Publ.*, 2002, **195**, 71–85.
19. Whitmarsh, R. B. *et al.*, Initial Reports of the Deep Sea Drilling Project, 23, Washington, US Government Printing Office, 1974.
20. Ajay, K. K., Chaubey, A. K., Krishna, K. S., Rao, D. G. and Sar, D., Seaward dipping reflectors along the SW continental margin of India: Evidence for volcanic passive margin. *J. Earth Syst. Sci.*, 2010, **119**, 803–813.
21. Tolán, T. L., Reidel, S. P., Beeson, M. H., Anderson, J. L., Fecht, K. R. and Swanson, D. A., Revisions to the estimates of the areal

extent and volume of the Columbia River Basalt Group. *Spec. Pap. Geol. Soc. Am.*, 1989, **239**, 1–20.

22. Storey, M., Mahoney, J. J., Saunders, A. D., Duncan, R. A., Kelley, S. P. and Coffin, M. F., Timing of hot spot-related volcanism and the breakup of Madagascar and India. *Science*, 1995, **267**, 852–855.
23. Gee, J. S., Diego, S. and Jolla, L., Source of oceanic magnetic anomalies and the geomagnetic polarity timescale. *Treatise Geophys.*, 2007, **5**, 455–507.
24. Muller, R. D., Royer, J. Y. and Lawver, L. A., Revised plate motions relative to the hotspots from combined Atlantic and Indian Ocean hotspot tracks. *Geology*, 1993, **21**, 275–278.

**ACKNOWLEDGEMENTS.** We are grateful to the Director, National Centre for Polar and Ocean Research (NCPOR), Goa, for the encouragement and support to carry out this work. We thank Dr K. A. Kamesh Raju, Visiting Scientist, NCPOR, for valuable discussions and suggestions which have improved the quality of the manuscript. We also thank Dr V. Yatheesh, CSIR-National Institute of Oceanography, Goa, for support and help. We are grateful to the Ministry of Earth Sciences (MoES), New Delhi for financial support through the EEZ Programme. Directorate General of Hydrocarbons, New Delhi is thanked for providing the multichannel seismic reflection sections used in the present study. We acknowledge the support received from the shipboard scientific party, officers and crew members of the cruise *MGS Sagar*. This is NPCOR contribution number J-48/2019-20.

Received 15 July 2019; revised accepted 17 December 2019

doi: 10.18520/cs/v118/i7/1118-1123

## Characteristics of Mesoproterozoic felsic meta-volcanics from the Shillong Group of rocks, Meghalaya, North East India

R. R. Naik<sup>1,\*</sup>, K. Theunuo<sup>1</sup>, T. K. Goswami<sup>2</sup>, M. A. Khonglah<sup>1</sup>, T. Pal<sup>1</sup> and S. K. Tripathy<sup>3</sup>

<sup>1</sup>Geological Survey of India, North Eastern Region, Shillong 793 003, India

<sup>2</sup>Department of Applied Geology, Dibrugarh University, Dibrugarh 786 004, India

<sup>3</sup>Regional Training Institute, Geological Survey of India, Eastern Region, Kolkata 700 091, India

**Shillong Group comprises a thick meta-volcano-sedimentary sequence forming a part of Shillong Plateau and Mikir Hills. The litho variants of felsic meta-volcanics are characterized in detail based on their constituent material, textural variation, depositional feature and mode of eruption. Lava flows are characterized as porphyritic, spherulitic and aphyric type whereas pyroclastic deposits are classified as tuff**

**breccia, lapilli tuff, tuff and ignimbrite. Fractured crystal and brecciated lithic fragments in tuff; fiamme and eutaxitic texture of ignimbrite suggest for sub-aerial eruption. The felsic meta-volcanics are rhyolitic to dacitic in composition and interbedded with tuffaceous phyllite, phyllite and quartzite.**

**Keywords:** Felsic volcanics, ignimbrite, lava flow, tuff, Shillong Group, subaerial.

THE Mesoproterozoic Shillong basin comprises a thick pile of meta-sedimentary sequence known as Shillong Group of rocks. It occupies the eastern central part of the Assam Meghalaya Gneissic Complex (AMGC) that forms part of the Shillong Plateau (Figure 1). The meta-sediments of Shillong Group are deposited unconformably over Umsning Schist Belt (USB)<sup>1</sup>. Sills and dykes of Khasi metabasics, Neoproterozoic granitoids of Pan-African origin (Myllem Granite (607 ± 13 Ma), South Khasi Granite (690 ± 19 Ma) and Kyrдем Granite (479 ± 26 Ma)) and late cretaceous mafic dykes and sills intrude the Shillong Group of rocks<sup>2–5</sup>. The Pan-African granitic plutons (South Khasi batholith) limit the upper age of Shillong Group to ~700 Ma and detrital zircon dates from quartzite of Shillong Group restricts the lower age limit to 1100 Ma (ref. 6). It has undergone polyphase deformation and metamorphosed under the green schist–amphibolite transitional facies<sup>7</sup>.

Felsic meta-volcanics in the form of meta-acid volcanic and tuff have been reported from Shillong Group as thin band of dark grey, fine-grained, intensely sheared and profusely impregnated with quartz veins occurring within phyllite<sup>1,8</sup>. Phenocryst of feldspar is strewn in the devitrified fine-grained groundmass. Volcanic tuff of Kerguelen hotspot-related volcanism exposed in Smit area is of Cretaceous age<sup>9</sup>. The felsic meta-volcanics of Shillong basin exposed in Meghalaya as well as in Mikir hills of Assam was least studied till date. Textural differences in the felsic lava flows from the Shillong basin exposed in Meghalaya part are reported here. The volcanic features of lava flows and pyroclastic deposits are reported here based on their constituent material, depositional feature and mode of eruption. Further, the nature of eruption and deposition of felsic meta-volcanics are also highlighted here.

The NE–SW trending meta-volcano-sedimentary sequences of the Shillong basin have regional dip towards SE. It covers approximately 2500 sq. km area of Shillong plateau. The litho sequence of Shillong Group was divided into three formations as Lower Mawlyndep, Middle Umiam and Upper Nongpiur formations (Table 1)<sup>1</sup>. The Lower Mawlyndep Formation comprises quartzite with subordinate quartz mica schist, phyllite and basal conglomerate at base. The Middle Umiam Formation dominantly comprises tuffaceous phyllite and felsic meta-volcanics with subordinate amount of phyllite,

\*For correspondence. (e-mail: mili27th@gmail.com)